J. Phys. C: Solid State Phys., **17** (1984) 6581–6599. Printed in Great Britain

A molecular dynamics simulation study of the orientationally disordered phase of sulphur hexafluoride

Martin T Dove† and G Stuart Pawley
Department of Physics, University of Edinburgh, Edinburgh EH9 3JZ, UK

Received 25 April 1984

Abstract. The orientationally disordered phase of sulphur hexafluoride at 150 K has been studied here using the molecular dynamics simulation technique, with particular emphasis placed on the origin and nature of the orientational disorder. A model involving the frustration of two competing intermolecular interactions that had been proposed previously has been shown to be a good description of the origin of the disorder through calculations that have given information concerning the correlations between the orientations of neighbouring molecules. It has also been shown that the disorder is dynamic rather than static in nature, and features of the molecular motion that are related to this dynamic disorder have been identified. It is suggested that some of the features of orientationally disordered crystals that have been studied might be observed experimentally in a coherent neutron scattering study, and some preliminary calculations of $S(\boldsymbol{Q})$ are reported.

1. Introduction

Sulphur hexafluoride exists in an orientationally disordered phase between 96 and 223 K that has previously been studied experimentally using the techniques of neutron scattering (Dolling *et al* 1979), Raman spectroscopy (Gilbert and Drifford 1972), LEED (Raynerd *et al* 1982) and NMR (Garg 1977). More recently, this phase and the other low-temperature phases have been studied using the molecular dynamics simulation (MDS) technique (Dove and Pawley 1983, Pawley and Dove 1983a, Pawley and Thomas 1982). SF_6 is of special interest in the study of orientational disorder in molecular crystals because it appears to represent one extreme of the range of the different symmetry properties of crystals that have orientationally disordered phases, with the crystal site symmetry being identical to the molecular symmetry. This is in contrast to molecular crystals such as the well-known alkali cyanides or ammonium halides in which the site symmetries of the molecular ions are higher than the symmetries of the molecular ions themselves. In these examples, the molecular ions reorientate between well defined sites that are symmetrically related but nevertheless distinct, with equal probability of occupancy in each site. It does not appear *a priori* that such distinct sites exist in the orientationally disordered phase of SF_6, at least not at temperatures well above the transitions to the more ordered low-temperature phases. Thus one might expect that the nature of the orientational disorder is different between these two extremes, but

† Present address: Department of Theoretical Chemistry, University Chemical Laboratories, Lensfield Road, Cambridge CB2 1EW, UK.

0022-3719/84/366581 + 19 $02.25

one might also expect that throughout the range of orientationally disordered crystals characteristics of both extremes might exist. For example, the case of C_2Cl_6 might well represent a small perturbation of the situation of SF_6, with the existence of distinct sites but with characteristics more representative of SF_6 (Gerlach *et al* 1983, 1984). It is therefore of importance to understand in detail the behaviour of the orientationally disordered phase of SF_6 at a microscopic level.

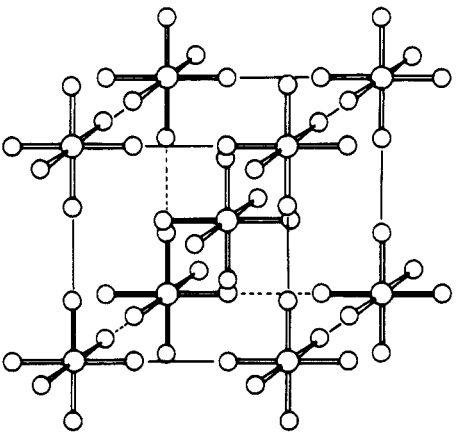

Figure 1. The crystal structure of SF_6 at 150 K showing the octahedral molecules in ordered orientations.

The experimental results cited above have shown that the structure of the orientationally disordered phase of SF_6 is body-centred cubic, with the molecules lying on the sites of octahedral symmetry with the S–F bonds preferentially aligned on average along the axes of the lattice cube, but with low barriers to molecular rotation (see figure 1). However, it is expected that a better understanding of the nature of this phase can be gained through MDS calculations. A model intermolecular potential for SF_6 that was proposed by Pawley (1981) has been used in a previous MDS study of SF_6 and it was shown that this model potential does indeed lead to the existence of an orientationally disordered phase in a temperature range roughly the same as that for the real system (Dove and Pawley 1983). In addition, two low-temperature phases were observed that appear to be in good qualitative agreement with the experimental data available (Pawley and Dove 1983a, Pawley and Thomas 1982). An analysis of the simulated orientationally disordered phase of SF_6 at 150 K showed that the molecules appear to have the same preferential alignment as observed experimentally, and an analysis of the single-particle dynamics demonstrated that the molecules exhibit the rotational diffusion that is characteristic of orientationally disordered crystals, with the molecular motions more akin to hindered rather than free rotation.

One of the advantages of computer simulations over laboratory experiments is that one has a prior knowledge of all the parameters that will determine the behaviour of the system under study, including the detailed form of the intermolecular potential. In the previous MDS study of SF_6 by Dove and Pawley (1983) it was possible to correlate the existence of the otientational disorder and the observed behaviour of the system to features of the intermolecular potential. It was found that the origin of the orientational

disorder is connected with the fact that there are two competing interactions that any molecule feels. The interaction between two nearest neighbours in the body-centred cubic lattice (i.e. between the two molecules situated on the corner and centre of the cubic non-primitive unit cell) favours the orientational order that is the time-averaged static structure of this phase, whereas the interaction between two next-nearest neighbours (i.e. between the two molecules situated at adjacent corners of the cubic cell) is strongly repulsive for this relative orientation. Thus there exists a frustration effect, which on cooling leads to two successive low-temperature phases which represent the static and dynamic compromises between these two competing interactions that is required by the lowering of the average kinetic energy per molecule. The existence of these phase transitions is in contrast to a possible alternative of a transition from the orientationally disordered phase to a structural analogue of a spin glass such as has been observed in other systems (Courtens 1983) and which is often the case where disorder in a high-temperature phase arises because of frustration.

The model discussed above poses several important questions to which the present paper is directed. The previous MDS study of SF_6 was concerned solely with the evaluation of single-particle and bulk properties, but also of interest is the nature of correlations between neighbouring molecules. In particular, one might expect that the effect of the frustration described above should be noticeable in the correlation between the orientations of next-nearest neighbours, and this feature is examined in the present study. Moreover, although the origin of the orientational disorder has been identified, the nature of the disorder remains to be properly characterised. Thus, in an attempt to distinguish between different possible descriptions of the nature of the disorder that will be discussed later, the single-molecule orientational distribution function has been re-examined in greater detail. Of further interest is the nature of the molecular motions and reorientations, and this has been studied in a qualitative manner by monitoring the orientations of two next-nearest-neighbour molecules as a function of time. The results of this study will be compared with those of the previous MDS study of SF_6, and it will be shown that a satisfactory description of both the origin and the nature of the orientationally disordered phase of SF_6 has now been obtained.

2. Simulation details

Many of the technical details associated with the present calculation have been discussed elsewhere (Dove and Pawley 1983, Pawley and Dove 1983b). The calculations have been performed on the ICL Distributed Array Processors (DAP) at the Edinburgh Regional Computer Centre. The DAP has a parallel architecture that has enabled the use of a large simulation sample of 4096 molecules. As in the previous MDS studies of SF_6 the intermolecular potential was modelled by using atom–atom Lennard-Jones potential functions for F . . . F interactions only, the effects of the S . . . S and S . . . F interactions being subsumed in this function. It has been shown (Dove and Pawley 1983) that this model potential is slightly softer than the true potential (due to the method of determining values for the parameters in the potential function), but as the consequences of this appear to be minimal no attempt has been made to improve the model. Since the calculations that are presented here were performed, an alternative set of Lennard-Jones potential parameters for SF_6 which give better agreement with experimental data on the structural second virial coefficient have been proposed by Powles *et al* (1983). The only intermolecular interactions that are taken into account explicitly are the

interactions between nearest and next-nearest neighbours. In this way the model retains only those features of the intermolecular interactions that are of significance as far as the phenomena under study are concerned, yet it is still of sufficient complexity to reproduce accurately many of the characteristics of the real SF_6 system, including the phase transitions to the low-temperature phases that are observed in nature. The equations of motion that were used in the simulation were those that generate a microcanonical ensemble, with a fixed volume chosen to correspond to a mean external pressure of approximately zero. The mean temperature of the MDS sample was 150 K, and the simulation was carried out for about 22300 time steps corresponding to a simulated time length of $\simeq 34$ ps.

Configurational analyses were carried out as the simulation proceeded, this being a more efficient procedure than storing the configurations generated every few time steps and performing the analyses at a later stage. For the calculation of distribution functions, a method of binning data that was proposed by Fincham (1983) and that is particularly efficient for use with the DAP was used. This method uses logical operations only, which are extremely fast on the DAP as the separate processing elements operate bit-serially, and so the process of repeatedly sorting data into 4096 bins did not noticeably increase the computational time.

3. Results

3.1. The orientational distribution function

The orientation of a molecule can be described either in terms of Euler angles or quaternions (Goldstein 1980), but these two representations have three and four separate parameters respectively, which make the representation of an orientational distribution function difficult. Thus in the present study the choice has been made to calculate the orientational distribution function of the S–F bonds, the orientation of each bond being fully described by the two polar coordinates $\{\theta, \varphi\}$. The orientational distribution function $f(\theta, \varphi)$ is defined so that the probability of any bond lying in an element of solid angle $d\Omega$ $(= \sin\theta \, d\theta \, d\varphi)$ in the direction $\{\theta, \varphi\}$ is given by $f(\theta, \varphi) \, d\Omega$. In the previous MDS study of the orientationally disordered phase of SF_6 the form of $f(\theta, \varphi)$ was given as averaged over all values of φ, but in the present calculation $f(\theta, \varphi)$ has been calculated over the whole space defined by $\{\theta, \varphi\}$, taking one symmetrically repeated octant $\{0 \leqslant \theta \leqslant \pi/2, 0 \leqslant \varphi \leqslant \pi/2\}$. The data are represented by a contour plot over $\{\theta, \varphi\}$ in figure 2, and figure 3 shows the form of $f(\theta, \varphi)$ along symmetry directions.

Two points should be noted. Firstly, $f(\theta, \varphi)$ has its maxima only along the directions of the cubic-unit-cell edges. One possible result of the model of competing interactions that has been described above might have been that $f(\theta, \varphi)$ would show additional maxima at orientations away from these symmetry directions, even to the point of suggesting that the orientational disorder in SF_6 is more akin to the situation in the ammonium halides or alkali cyanides discussed earlier with the SF_6 molecules orientated within different distinct sites with reorientations of the molecules between these sites, leading to an effective site symmetry different to that of the molecule†. This however

† Such a difference would not have been observed in the analysis of neutron diffraction data of Dolling *et al* (1979) since it would correspond to terms in the harmonic expansion of $f(\theta, \varphi)$ that were not included in the structure refinement, and additional maxima in $f(\theta, \varphi)$ would probably not be resolveable in the representation shown earlier by Dove and Pawley (1983) that had been averaged over φ.

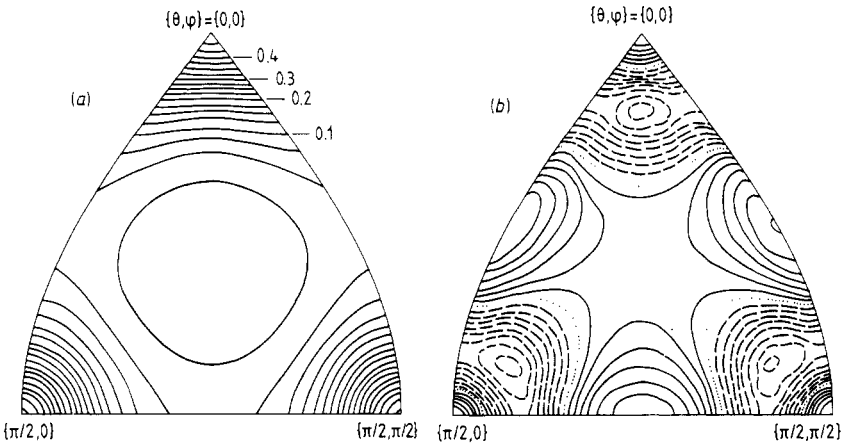

Figure 2. The orientation distribution function for S–F bonds $f(\theta, \varphi)$ as a function of the polar angles θ and φ shown as a contour plot (*a*). The difference between this distribution and a simple gaussian distribution as described in the text is shown in (*b*), where negative regions are shown as broken contours. In these representations small elements of equal area correspond to equal values of solid angle.

does not appear to be the case, and instead the molecules librate about the orientation of the unit-cell axes. The second point is that the maxima in $f(\theta, \varphi)$ are slightly extended towards the (110) direction in a manner that is consistent with the existence of molecular rotations about symmetry directions that will be discussed later.

In order to highlight aspects of the disorder we have fitted a model probability distribution function to $f(\theta, \varphi)$ that consists of a sum of three Gaussians, each one centred along the different crystal axes and dependent only upon the angle between the S–F bond and the closest axis. Because this model distribution function is normalised, the only adjustable parameter is the width of the Gaussians, and the best fit to $f(\theta, \varphi)$ was obtained with a half width at half height of 17.15°. This model represents what would be the case if the molecules were librating in a harmonic potential, and the large discrepancies between the model and the calculated $f(\theta, \varphi)$ show that the motions of the

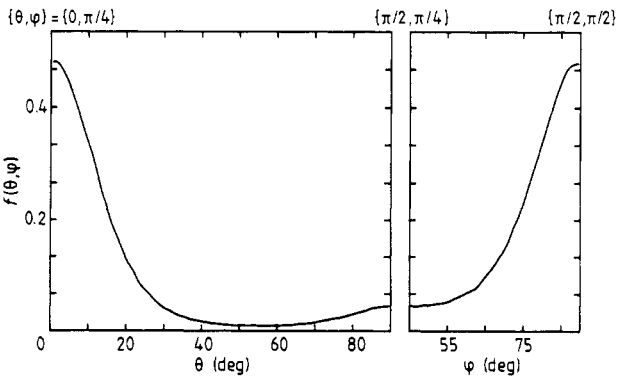

Figure 3. The form of $f(\theta, \varphi)$ along symmetry directions.

SF_6 molecules are not harmonic. In particular, $f(\theta, \varphi)$ is significantly larger than the Gaussian model in regions far away from the crystal axes.

Hohlwein (1981) has refined the structure of SF_6 from the neutron diffraction data of Dolling *et al* (1979) using this Gaussian model. He obtained a value for the half width of $16.6 \pm 0.6°$, but found however that the refinement was relatively insensitive to departures from this simple model.

3.2. Analysis of fluorine–fluorine contact distances

In the model of competing interactions that was described above, the interaction that acts to oppose orientational order is the interaction between next-nearest-neighbouring molecules (Dove and Pawley 1983). This interaction is strongly repulsive for two orientationally ordered molecules positioned at the lattice sites (i.e. at adjacent unit-cell corners) because of the close contact of the two fluorine atoms that lie along the vector joining the two molecular centres of gravity. At 150 K and zero pressure the cubic-unit-cell length for the simulation sample of SF_6 is 5.764 Å which, with an S–F bond length of 1.565 Å, leads to a fluorine–fluorine contact distance r_c of 2.634 Å if the two

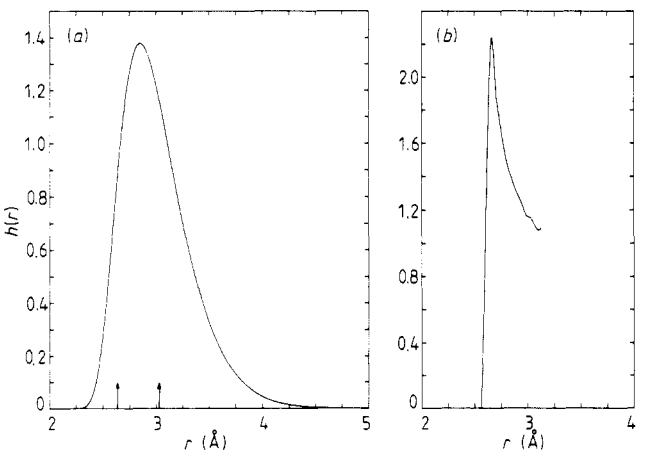

Figure 4. The probability distribution function $h(r)$ for close F. . .F contact distances r. (*a*) observed in the simulations and (*b*) calculated from $f(\theta, \varphi)$ assuming no correlations between the orientations of neighbouring S–F bonds.

molecules are orientationally ordered. The value for the Lennard-Jones radius used in the potential function employed in the present study was 2.7 Å for which a pair-wise equilibrium F. . .F contact distance r_0 would be 3.031 Å. Thus it is expected that next-nearest neighbours would either reorientate or move apart in order to increase the F. . .F contact distance along the intermolecular vector. In the moving apart process orientational disorder would still arise because of the decrease in the corresponding contact distances between the other next-nearest neighbours in the directions of motion. From a calculation of the next-nearest-neighbour close-F. . .F-contact distances, a probability distribution function $h(r)$ analogous to a radial distribution function has been calculated, and this is shown in figure 4(*a*). It should be noted that only these contacts have been included; $h(r)$ is not a general radial distribution function for all F. . .F distances. It can

be seen that very few contact distances lie close to the ordered distance r_c, and the calculated mean contact distance $r_M = 3.011$ Å is very close to the equilibrium contact distance r_0. That r_M is slightly shorter than r_0 is probably related to the fact that there is additional attraction between these two neighbouring atoms that arises because of the interactions between one atom and all of the other atoms of the second molecule. The form of $h(r)$ strongly indicates that the strong repulsions between the two nearest fluorine atoms of next-nearest neighbours does lead to the molecules moving in order to increase the F. . .F contact distance to a more stable value consistent with the prediction of the frustration model.

In order to confirm that the form of $h(r)$ is at least partly due to these correlation effects a corresponding distribution function was calculated from $f(\theta, \varphi)$ assuming no correlations between the orientations of neighbouring S–F bonds and neglecting any relative translational motions (which might be expected to be small in any case). We call this corresponding distribution function an 'uncorrelated distribution function'. The resultant graph of $h(r)$ is given in figure 4(b). This function has only been calculated for values of r smaller than 3.2 Å because for greater contact distances it would be necessary to include the contributions from S–F bonds that have $\theta > 45°$, and data obtained from $f(\theta, \varphi)$ for this case are ambiguous since $f(\theta, \varphi)$ is a bond orientational distribution function rather than a molecular orientational distribution function. In the case where $\theta > 45°$, the relevant features of the molecular orientation cannot be defined in a unique manner. It can be seen that the observed and uncorrelated distribution functions are very different; in particular, the uncorrelated distribution function peaks strongly at low values of r, corresponding to a high probability of the alignment of both of the neighbouring bonds, and the mean F. . .F contact distance is 2.933 Å, 0.1 Å shorter than observed and leading to repulsive forces. Thus it can be safely concluded that the observed form of $h(r)$ shows strong evidence for steric repulsion of the closest next-nearest-neighbour S–F bonds due to the short contact distance between the fluorine atoms.

3.3. Correlations between next-nearest neighbours

The results discussed in the previous section have shown that the orientations of next-nearest-neighbour molecules are correlated in such a manner that the two closest S–F bonds repel each other away from the orientationally ordered state. It is therefore expected that the most important effects of this correlation should be seen in the correlation between the orientations of the two closest S–F bonds of the next-nearest-neighbouring molecules. We have defined a distribution function $g(\Theta, \Phi)$ exactly analogous to $f(\theta, \varphi)$, with the variables $\{\Theta, \Phi\}$ related to the polar coordinates $\{\theta_1, \varphi_1\}$ and $\{\theta_2, \varphi_2\}$ of the two bonds by

$$\Theta = \theta_1 + \theta_2 \qquad \Phi = |\varphi_1 - \varphi_2|.$$

It should be noted that the representation of the correlations under study via a distribution function such as $g(\Theta, \Phi)$ does have limitations. For example, as stated above, such correlations might be expected to have a position dependence that has not been taken into account here.

The form of $g(\Theta, \Phi)$ calculated in the simulation is shown in figure 5(a) as a contour plot. The function $g(\Theta, \Phi)$ peaks strongly for $\Theta = 26°$, with the peak elongated along Φ with its largest value at low Φ. $g(\Theta, \Phi)$ falls to zero for $\Theta = 0$, a configuration that corresponds to the orientational ordering of the two molecules. Similarly $g(\Theta, \Phi)$ also

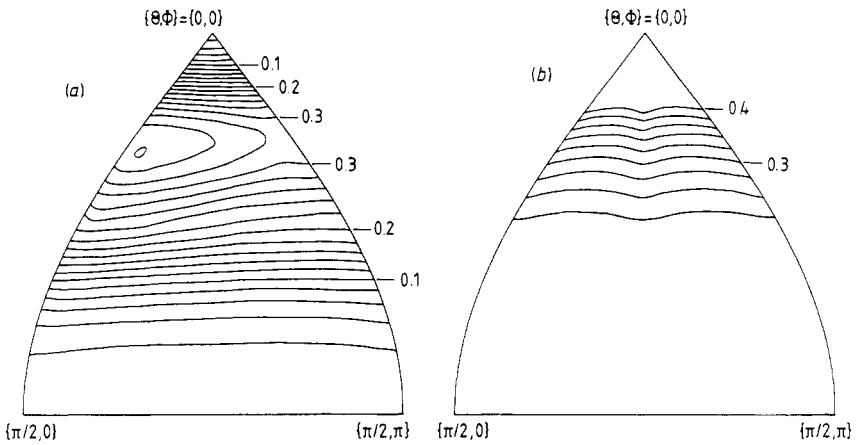

Figure 5. Contour representation of the correlation distribution function $g(\Theta, \Phi)$. (*a*) as observed in the simulations and (*b*) as calculated from $f(\theta, \varphi)$ assuming no correlations between the orientations of neighbouring S–F bonds. The variables are defined in the text.

falls to zero at large values of Θ, consistent with the form of the single-molecule orientation distribution $f(\theta, \varphi)$. The interesting point is that the existence of the elongated peak implies that many pairs of molecules have one molecule aligned with one S–F bond lying along the unit-cell axis in the direction of the neighbouring molecule and with the neighbouring molecule aligned so that the close S–F bond lies 26° away from the intermolecular vector. If the molecular centres of mass lie on the lattice sites, the F. . .F contact distance for this relative orientation is 2.89 Å, which can be compared with the distance corresponding to the maximum in $h(r)$ of 2.85 Å.

The conclusions drawn here were checked in the same way as in the analysis of the F. . .F contact distance distribution function $h(r)$ by forming an uncorrelated distribution function similar to $g(\Theta, \Phi)$ from the single-molecule bond orientational distribution function with the assumption of no neighbour correlations; this is shown in figure 5(*b*). For the same reason that the range of values of the uncorrelated form of $h(r)$ that could be calculated was limited, the uncorrelated form of $g(\Theta, \Phi)$ was limited to $\Theta < 45°$. As in the case of $h(r)$, the principal difference between the observed and uncorrelated forms of $g(\Theta, \Phi)$ is that the ridge in the uncorrelated distribution function lies along $\Theta = 0$ whereas the corresponding feature is actually observed to lie away from this point. This difference shows that the observed distribution function is indeed strongly indicative of the existence of significant correlations between the orientations of the closest neighbouring S–F bonds.

3.4. The rotational motions of molecules

Further information concerning the nature of the orientational disorder in SF_6 can be obtained by investigating the rotational motions of the molecules. For this purpose the positions of the fluorine atoms of two molecules that are next-nearest neighbours in the crystal have been recorded as a function of time. The results of this are shown in figure 6, where the coordinates have been defined with respect to a set of cartesian axes that have the same orientation as the cubic lattice and with the x direction lying along the vector that joins the lattice sites of the two molecules. Only three atoms for each molecule

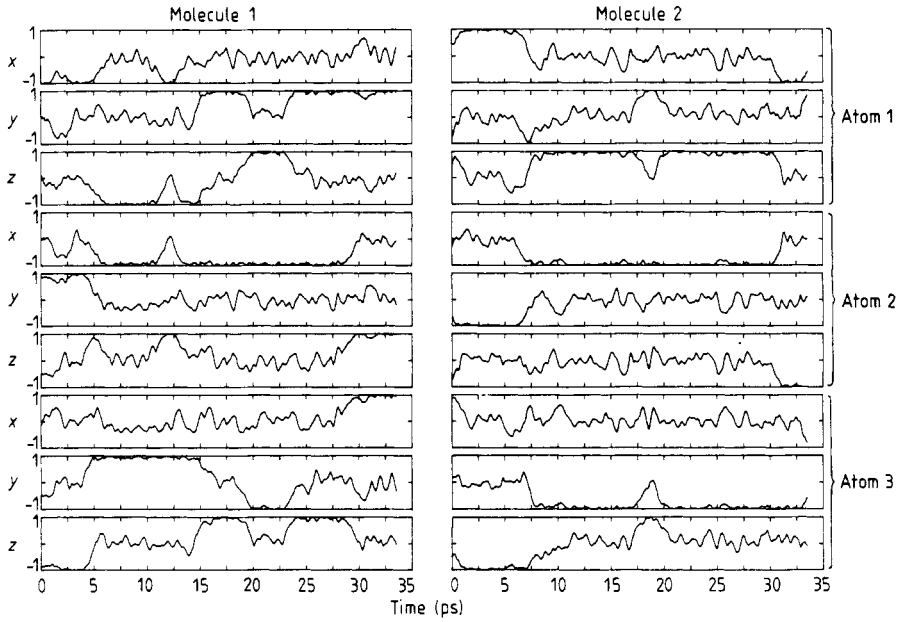

Figure 6. The motion of the fluorine atoms of two next-nearest-neighbouring SF_6 molecules as a function of time. The coordinates are scaled and are taken relative to a set of cartesian axes aligned with the axes of the crystal unit cell and with the origins at the centres of the molecules.

are shown since the remaining three are related to those shown by inversion symmetry, and the coordinates of the atoms are given with respect to the positions of the sulphur atoms and scaled by dividing by the S–F bond length (1.565 Å). Although any conclusions drawn from figure 6 are of qualitative significance only, the following points should be noted.

(i) On average, the molecules are orientated in accord with the calculated form of the single-molecule orientational distribution function $f(\theta, \varphi)$ (figure 2), with the S–F bonds lying close to the direction of the cubic-unit-cell edges.

(ii) The molecules remain in a particular orientation for an approximate average

Table 1. The reorientations of molecules during the time evolution of the simulation of the orientationally disordered phase of SF_6 at 150 K. The time refers to the time that one of the two molecules being monitored underwent a reorientation jump, with the origin corresponding to the start of the simulation run. The second and third columns give the axes of rotations.

Time (ps)	Molecule 1	Molecule 2
5	$(\bar{1}1\bar{1}$	
7		$(\bar{1}\bar{1}\bar{1})$
13.5	$(\bar{1}00)$	
19.5	$(\bar{1}00)$	
23.5	(100)	
29	(010)	
30.5		$(0\bar{1}0)$

time of 5.5 ps before undergoing a large reorientation to another symmetrically equivalent orientation. The time taken to reorientate is of the order of 2 ps.

(iii) The reorientational motions correspond to rotations about axes that lie along symmetry directions of the unit cell. The details of the observed 'permanent' reorientations are given in table 1, from which it can be seen that the predominant type of reorientation consists of a rotation about the fourfold-symmetry axis. There are also two observed events in which the molecules undergo a complete 90° jump about a fourfold axis but then immediately undergo a reverse jump.

(iv) Between reorientations the molecules librate about the symmetry orientations with large amplitudes of about 15°. The magnitude of this amplitude is consistent with the spread of the maxima in the single-molecule orientation distribution function (§ 3.1).

This analysis cannot be used to indicate any cooperative motion as the number of observed reorientations is small, and more molecules would need to be considered. A formal analysis of correlated molecular reorientations will be presented elsewhere. However, the single-particle motions are well represented by figure 6.

3.5. Single-molecule rotational potential

A single molecule will experience a potential that is obviously determined by the instantaneous positions and orientations of that molecule and of all of its neighbours. In principle it may be possible to separate out a term that depends solely upon the orientation of the molecule, known as the single-molecule rotational potential (Press 1981). This term is then itself separable into two parts, a static (time-averaged) and a fluctuating part, and the characteristics of the dynamics of a single molecule are related to the relative magnitudes of these two contributions. As noted above, in a simulation study one has an *a priori* knowledge of the form of the intermolecular potential so it is possible to obtain direct information concerning the single-molecule rotational potential. This has been calculated for SF_6 by replacing a single molecule by a reference molecule and calculating the potential seen by that molecule for a number of different orientations. This procedure was carried out for all molecules for a number of different configurations generated during the simulation in order to obtain a mean static potential and a reliable estimate of the mean of the square of the fluctuations in that potential. An obvious problem is the choice of position for the centre of mass of the reference molecule. It was decided to use the positions of the molecules being replaced, the justification for this choice being that a displacement of a molecule will generally be accompanied by a similar displacement of its neighbours. This cooperative motion will correspond to the eigenvector of a long-wavelength acoustic phonon, the amplitude of which, being inversely proportional to the frequency, is expected to be larger than that for other modes of vibration such as the acoustic modes with wavevectors that lie close to the boundaries of the Brillouin zone. Calculations using the lattice sites as the positions of the reference molecules were also performed, and the results of these indicated that the former choice for the positions of the molecules was justified. The validity of this choice is also confirmed by the fact that the calculated mean potential for the completely ordered orientation of the reference molecule ($-17.406\ \mathrm{kJ\,mol^{-1}}$) was closer to the equilibrium value ($-20.7\ \mathrm{kJ\,mol^{-1}}$; Dove and Pawley 1983) than the magnitude of the fluctuations of the potential. Another problem is that part of the fluctuation in the potential arises through the fluctuation in the mean potential energy of the sample. This gives a contribution to the single-molecule potential with a variance that is proportional

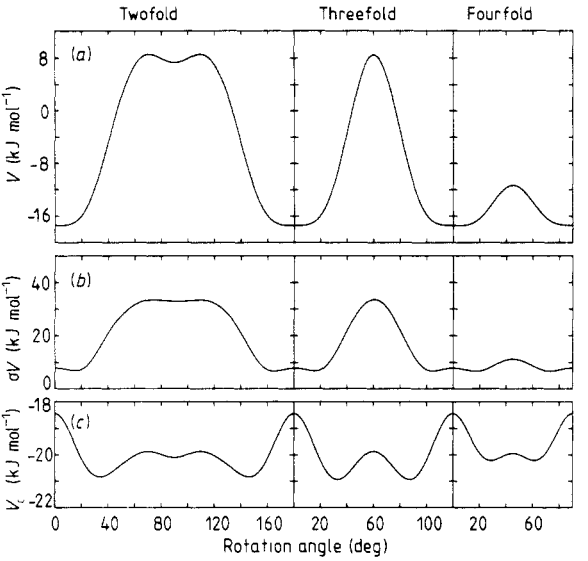

Figure 7. (*a*) Mean single-molecule rotational potential energy V, (*b*) standard deviation of the single-molecule rotational potential energy σV, and (*c*) single-molecule potential energy for a static ordered structure V_c as functions of molecular orientations for rotations about the two-, three- and fourfold-symmetry axes.

to N^{-1}, where N is the number of particles in the sample. Although such a contribution will be negligible in a macroscopic crystal where $N \sim 10^{24}$, it is not immediately obvious that this will prove to be the case in a simulation where the number of molecules is as small as 4096.

The results of these calculations are given in figure 7, where the static potential and its standard deviation (a measure of the amplitude of the fluctuating contribution to the potential) is shown for molecular rotations about the two-, three- and fourfold-symmetry axes. Also shown in this figure is the corresponding calculation for a hypothetical completely ordered crystal. It can be seen that the fluctuations in the potential are larger than the standard deviation of the potential of the whole sample (0.019 kJ mol^{-1}; Dove and Pawley 1983), so the problem of the size dependence of the fluctuating potential is not in fact important. These results show the existence of potential barriers between symmetrically equivalent orientations related by rotations about the symmetry axes considered, and also show that there is a strong fluctuating potential with an amplitude that is comparable with the heights of the potential barriers. The barrier to rotation about the fourfold axis is considerably smaller than for other rotations, a result that might have been anticipated in the light of the results given in the previous section. It is of interest to note that any possible potential minima of the type described in previous sections with the positions of the minima lying at angles away from the directions of the unit-cell axes do not appear to exist. This is consistent with the other results described in the present paper.

In connection with this latter point it can be seen that the rotational potential in the hypothetical ordered structure shows very different features to the observed potential. In particular, the minima in the hypothetical potential do not occur at the symmetric orientations. It may be of relevance that the positions of the minima in the ordered

structure (at rotation angles of $\simeq 30°$) show similarities to the results for the correlations of the orientations of next-nearest-neighbour molecules described above, with a tendency for some of the S–F bonds to be aligned along the unit-cell axes with the closest bonds on the neighbouring molecules lying at angles of 26°.

The results of this section are very similar to the calculated form of the effective single-molecule rotational potential in the orientationally disordered phase of C_2Cl_6 obtained from neutron diffraction data by Gerlach *et al* (1984). In particular, in this material the minima correspond to the chlorine pseudo-octahedra being oriented with the atoms lying close to the crystal axes with the lowest potential barriers to reorientation corresponding to rotations about the approximate four fold axes.

4. Discussion

The questions posed in § 1 can effectively be condensed into two major ones: what is the microscopic origin of the orientational disorder, and what is the nature of this disorder? On the basis of an *a priori* knowledge of the intermolecular potential, we (Dove and Pawley 1983) proposed that the disorder arises as a result of a competition between two types of intermolecular interaction: an orientational ordering interaction between nearest neighbours, and a repulsive and hence disordering interaction between next-nearest neighbours. The effects of this frustration have been clearly seen in the calculations of correlation effects between next-nearest neighbours (§§ 3.2 and 3.3), demonstrating that the SF_6 molecules reorient away from the orientation of the cubic crystal-site symmetry in order to increase the contact distance between the closest neighbouring fluorine atoms. This has raised the possibility that the relaxed (i.e. thermally equilibrated) crystal might contain well defined potential wells for the molecular orientations that are slightly away from the symmetric orientation as suggested by the static calculation (figure 7(*b*)) with the disorder arising from the existence of more sites per molecule than the number of equivalent orientations, but such potential wells do not appear to exist. Instead, the only molecular sites are those with the symmetry of the unit cell, and thus the disorder is purely dynamic, with the molecules moving in response to general forces and the frustration effects outlined above, with the next-nearest-neighbouring molecules moving in such a way that the closest F. . .F contact distances are increased from the orientationally ordered values to stable equilibrium values.

In the absence of static disorder it is reasonable to question the meaning of the term 'disorder' and to ask whether in fact all that this term conveys is the existence of large-amplitude (and hence strongly anharmonic) librations. The answer to this is essentially contained in the preceding discussion. The frustration effects will mean that even at very low temperatures (hypothetically assuming that no transition to another phase occurs) the molecules will not be orientationally ordered as they would be if the crystal was just anharmonic. Thus the ground state will still realise the forms of the neighbour distribution functions given in the previous sections. To put it another way that avoids considering a hypothetical ground state, it would be expected that the variation of the mean square angle of the S–F bonds with respect to their closest crystal axes would not vary linearly with temperature extrapolating to zero at 0 K (neglecting quantum effects) but would decrease to a significant value at 0 K. We believe that this is the main characteristic that distinguishes genuine disorder from simple large-amplitude fluctuations in a crystal such as SF_6 in which there is no static component of the disorder such as exists in some other orientationally disordered crystals. Alternatively, other features

characteristic of orientational disorder are rotational diffusion and frequent large molecular reorientations, both of which are observed in SF_6, but these features are hard to quantify in the limits of large-amplitude fluctuations and strong anharmonicities.

The model of the dynamic orientational disorder in SF_6 is consistent with the results of measurements of properties associated with the single-molecule dynamics. The power spectrum for rotational motions calculated by Dove and Pawley (1983) and reproduced in figure 8 shows that there are no well defined excitations associated with the rotational motion (i.e. optic modes), and that there is significant rotational diffusion. This feature is itself consistent with the measurement of large fluctuations in the single-molecule rotational potential (Press 1981) and is also revealed in the study of the rotational motion of single molecules (§ 3.4). The molecules execute large-amplitude librations about effectively unstable orientations, driven by large fluctuating forces which occasionally cause complete reorientation, and the collective motion is more diffusion-like than phonon-like.

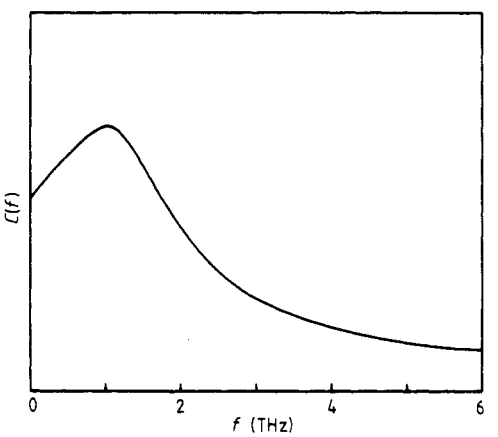

Figure 8. The power spectrum $C(f)$ associated with the angular velocity autocorrelation function for SF_6 (after Dove and Pawley 1983).

5. Calculation of the neutron scattering $S(\boldsymbol{Q})$

On the basis of the few comparisons with corresponding experimental results that are possible we believe that the results of the MDS calculations for the orientationally disordered phase of SF_6 will be in good agreement with the behaviour in the orientationally disordered phase of the real SF_6 crystal. One obvious way of observing the effects of the orientational disorder would be through coherent neutron scattering measurements. Accordingly we have calculated the total scattering function $S(\boldsymbol{Q})$, as would be measured in a 'total scattering' experiment.

The total scattering function $S(\boldsymbol{Q})$ for wavevector transfer $\boldsymbol{Q}$ is given by

$$S(\boldsymbol{Q}) = \left\langle \left| \sum_i R_i U_i \beta_i \right|^2 \right\rangle$$

where

$$R_i = \exp(i\boldsymbol{Q} \cdot \boldsymbol{R}_i)$$

$$\beta_i = \sum_{\mu} b_\mu \exp(i\boldsymbol{Q} \cdot \boldsymbol{r}_{i\mu})$$

$$U_i = \exp(i\boldsymbol{Q} \cdot \boldsymbol{u}_i)$$

and $\boldsymbol{R}_i$ is the equilibrium (lattice) position of the centre of mass of the ith molecule, $\boldsymbol{u}_i$ is an instantaneous displacement of that molecule and $\boldsymbol{r}_{i\mu}$ is the instantaneous position of the μth atom of the ith molecule with respect to the position of the centre of mass of the molecule (i.e. $\boldsymbol{R}_i + \boldsymbol{u}_i$). The scattering length of the μth atom is b_μ, and the angle brackets denote a thermal average. It is possible to express $S(\boldsymbol{Q})$ as a sum of separate contributions:

$$S(\boldsymbol{Q}) = \sum_{m=1}^{6} S_m(\boldsymbol{Q})$$

where the expressions for the six separate contributions are given in table 2. The two terms $S_1(\boldsymbol{Q})$ and $S_2(\boldsymbol{Q})$ arise from the positional and orientational disorder of single molecules respectively, and $S_4(\boldsymbol{Q})$ and $S_5(\boldsymbol{Q})$ are the terms that give information concerning the correlations between the relative displacements and orientations of neighbouring molecules. $S_3(\boldsymbol{q})$ is a term that is closely related to the Bragg scattering intensity and that becomes equivalent to it if the positions and orientations of a molecule are uncorrelated, i.e. if

$$\langle \beta_i U_i \rangle = \langle \beta_i \rangle \langle U_i \rangle.$$

Because of the inversion symmetry of the SF_6 molecule it might be expected that this coupling does not exist to first order, but in the previous MDS calculation of the orientationally disordered phase of SF_6 (Dove and Pawley 1983) it was shown that at larger values of $|\boldsymbol{Q}|$ this coupling is not insignificant. However, at any point in reciprocal space away from a Bragg point $S_3(\boldsymbol{Q})$ is identically zero and so the extent of this coupling is unimportant. The sixth contribution $S_6(\boldsymbol{Q})$ arises from the correlations between the relative orientations and displacements of neighbouring molecules. This is the important term in any investigation of rotation–translation coupling in a molecular crystal.

A similar analysis of the structure of $S(\boldsymbol{Q})$ for an orientationally disordered molecular crystal has been given by Kobashi and Etters (1982), the difference being that these authors took both $S_4(\boldsymbol{Q})$ and $S_6(\boldsymbol{Q})$ to be equal to zero by assuming that the molecular displacements can be expressed using simple Debye–Waller factors and that the coupling between the translational and rotational motions is negligible. This latter assumption might in fact be expected to fail in many orientationally disordered crystals in view of the important role that this mechanism plays in the phase transitions to low-temperature ordered phases (see e.g. Michel 1984). Kobashi and Etters (1982) also showed how the contributions to $S(\boldsymbol{Q})$ that depend on the molecular orientations could be re-expressed in terms of appropriate symmetry-adapted harmonics. It is straightforward to write down the corresponding terms for SF_6, and in fact the use of quaternions instead of Euler angles as in the MDS program greatly simplifies the form of the Wigner rotational matrices used by Kobashi and Etters, but we do not pursue such an analysis here.

The six contributions to $S(\boldsymbol{Q})$ are easily programmed for MDS calculations, although the products of two site–site averages in the expressions for S_4 and S_6 necessitate the storage of separate accumulating sums for each neighbouring pair of molecules through-

Table 2. The total scattering factor $S(\boldsymbol{Q})$ expressed as a sum of six contributions:

$$S(\boldsymbol{Q}) = \sum_{m=1}^{6} S_m(\boldsymbol{Q}).$$

Here the prime denotes the exclusion of the terms for $i = j$, and $\boldsymbol{R}_{ij} = \boldsymbol{R}_i - \boldsymbol{R}_j$, $\boldsymbol{u}_{ij} = \boldsymbol{u}_i - \boldsymbol{u}_j$, and $\boldsymbol{r}_{iuiv} = \boldsymbol{r}_{iu} - \boldsymbol{r}_{iv}$. All other symbols are defined in the text, as also are the physical meanings of the separate $S_m(\boldsymbol{Q})$.

$$S_1(\boldsymbol{Q}) = \sum_i \left| \sum_u b_u \langle \exp(i\boldsymbol{Q} \cdot \boldsymbol{r}_{iu}) \rangle \right|^2 - \sum_i \left| \langle \exp(i\boldsymbol{Q} \cdot \boldsymbol{u}_i) \rangle \sum_u b_u \langle \exp(i\boldsymbol{Q} \cdot \boldsymbol{r}_{iu}) \rangle \right|^2$$

$$S_2(\boldsymbol{Q}) = \sum_i \sum_{uv} b_u b_v [\langle \exp(i\boldsymbol{Q} \cdot \boldsymbol{r}_{iuiv}) \rangle - \langle \exp(i\boldsymbol{Q} \cdot \boldsymbol{r}_{iu}) \rangle \langle \exp(-i\boldsymbol{Q} \cdot \boldsymbol{r}_{iv}) \rangle]$$

$$S_3(\boldsymbol{Q}) = \left| \sum_i \langle \exp(i\boldsymbol{Q} \cdot \boldsymbol{u}_i) \rangle \exp(i\boldsymbol{Q} \cdot \boldsymbol{R}_i) \sum_u b_u \langle \exp(i\boldsymbol{Q} \cdot \boldsymbol{r}_{iu}) \rangle \right|^2$$

$$S_4(\boldsymbol{Q}) = \sum_{ij}{}' \exp(i\boldsymbol{Q} \cdot \boldsymbol{R}_{ij}) [\langle \exp(i\boldsymbol{Q} \cdot \boldsymbol{u}_{ij}) \rangle - \langle \exp(i\boldsymbol{Q} \cdot \boldsymbol{u}_i) \rangle \langle \exp(-i\boldsymbol{Q} \cdot \boldsymbol{u}_j) \rangle] \times \sum_{uv} b_u b_v \langle \exp(i\boldsymbol{Q} \cdot \boldsymbol{r}_{iuiv}) \rangle$$

$$S_5(\boldsymbol{Q}) = \sum_{ij}{}' \exp(i\boldsymbol{Q} \cdot \boldsymbol{R}_{ij}) \langle \exp(i\boldsymbol{Q} \cdot \boldsymbol{u}_i) \rangle \langle \exp(-i\boldsymbol{Q} \cdot \boldsymbol{u}_j) \rangle \sum_{uv} b_u b_v [\langle \exp(i\boldsymbol{Q} \cdot \boldsymbol{r}_{iujv}) \rangle - \langle \exp(i\boldsymbol{Q} \cdot \boldsymbol{r}_{iu}) \rangle \langle \exp(-i\boldsymbol{Q} \cdot \boldsymbol{r}_{jv}) \rangle]$$

$$S_6(\boldsymbol{Q}) = \sum_{ij}{}' \exp(i\boldsymbol{Q} \cdot \boldsymbol{R}_{ij}) \sum_{uv} b_u b_v [\langle \exp(i\boldsymbol{Q} \cdot \boldsymbol{u}_{ij}) \exp(i\boldsymbol{Q} \cdot \boldsymbol{r}_{iuiv}) \rangle - \langle \exp(i\boldsymbol{Q} \cdot \boldsymbol{u}_{ij}) \rangle \langle \exp(i\boldsymbol{Q} \cdot \boldsymbol{r}_{iujv}) \rangle]$$

out the MDS run, and the calculations are somewhat time-consuming because of the lack of parallelism in the problem (e.g. in the calculations of the site–site averages). In the present study the scattering lengths used for the sulphur and fluorine atoms were those that correspond to experimental values, and $S(\boldsymbol{Q})$ was evaluated for 64 values of $\boldsymbol{Q}$ lying in the $(1\bar{1}0)$ plane. It was necessary to take account of the fact that the small (compared with a real macroscopic crystal) size of the MDS sample greatly restricts the range of meaningful $\boldsymbol{Q}$-values. The final values of $S(\boldsymbol{Q})$ were obtained from averaging over configurations analysed every 0.3 ps during a simulation run lasting for 48 ps. The accuracies of the final values of the contributions to $S(\boldsymbol{Q})$ were estimated by comparing the results from the two halves of the simulation time. It should be noted that away from the Bragg points the standard deviation of the total $S(\boldsymbol{Q})$ is in general of the same size as $S(\boldsymbol{Q})$ itself. That this relative size of the standard deviation simply arises from the thermal fluctuations (or phonons) can be easily demonstrated by calculating $S(\boldsymbol{Q})$ for a one-dimensional chain of atoms that is vibrating with the lowest harmonic frequency. In this case, the calculated values of $S(\boldsymbol{Q})$ have similar standard deviations to those calculated for the three-dimensional SF_6. Of course, this corresponding variance corresponds to the analysis of instantaneous configurations and not to the time averaging that would be observed in a neutron scattering experiment where the sampling time associated with neutron scattering from a crystal is much longer than in a simulation study.

The results from the calculations of $S(\boldsymbol{Q})$ are given in table 3. A number of points can be seen.

(i) The intensities of the Bragg peaks are in good agreement with those measured in the neutron diffraction experiment of Dolling *et al* (1979), taking into account the fact

Table 3. The calculated values for the six contributions to $S(\boldsymbol{Q})$ and the total value for SF_6 at 150 K, calculated for 64 values of $\boldsymbol{Q}$. The definitions of the separate contributions are given in table 2 and explained in the text. The estimated errors are given in brackets.

h	k	l	S_1	S_2	S_3	S_4	S_5	S_6	Total S
0	0	0	0 (0)	0 (0)	222291200 (0)	8385978 (4051398)	0 (0)	−8385978 (4051398)	222291200 (0)
0	0	2	505 (6)	1525 (4)	5599174 (37266)	208010 (97643)	−566 (120)	−110401 (100737)	5698246 (40239)
0	0	4	8960 (48)	5541 (24)	14689608 (287835)	548914 (250411)	−706 (67)	112751 (302234)	15365064 (339568)
0	0	6	290 (10)	7177 (4)	78629 (809)	3214 (1666)	−36 (74)	13622 (373)	102897 (1171)
0.25	0.25	0	461 (5)	0 (0)	0 (0)	−2035 (950)	0 (0)	1824 (881)	251 (63)
0.25	0.25	2	353 (2)	1712 (1)	0 (0)	100 (10)	−345 (133)	23 (254)	1844 (376)
0.25	0.25	4	8361 (36)	5529 (15)	0 (0)	2537 (1120)	−436 (20)	−350 (1681)	15641 (520)
0.25	0.25	6	323 (11)	7224 (7)	0 (0)	33 (16)	14 (10)	−1086 (28)	6507 (72)
0.5	0.5	0	1274 (15)	1 (0)	0 (0)	−2294 (644)	0 (0)	1270 (609)	250 (21)
0.5	0.5	2	66 (0)	2205 (3)	0 (0)	−45 (47)	−351 (152)	−229 (37)	1646 (65)
0.5	0.5	4	6794 (20)	5421 (3)	0 (0)	−1434 (770)	−421 (428)	−180 (426)	10180 (786)
0.5	0.5	6	423 (11)	7343 (2)	0 (0)	−39 (1)	−46 (34)	335 (755)	8016 (708)
0.75	0.75	0	1895 (22)	1463 (2)	0 (0)	−1770 (534)	−228 (97)	585 (848)	1945 (240)
0.75	0.75	2	68 (3)	2879 (1)	0 (0)	46 (16)	313 (180)	−849 (386)	2457 (226)
0.75	0.75	4	4811 (7)	5112 (5)	0 (0)	1598 (2010)	−100 (10)	1304 (187)	12726 (2220)
0.75	0.75	6	577 (10)	7485 (8)	0 (0)	115 (146)	−23 (6)	−195 (1336)	7959 (1183)
1	1	0	773 (8)	121 (0)	19199376 (30683)	721510 (349361)	−15 (20)	−750682 (348967)	19171056 (30253)
1	1	2	765 (17)	3660 (9)	5247507 (18903)	195290 (94293)	541 (162)	−226445 (79357)	5221317 (34010)
1	1	4	2996 (0)	4587 (6)	3995168 (109406)	150013 (69023)	244 (217)	−9961 (112622)	4143045 (152782)
1	1	6	742 (7)	7585 (16)	171292 (6280)	6832 (3596)	9 (45)	20583 (14574)	207042 (11926)
1.25	1.25	0	84 (1)	526 (2)	0 (0)	−57 (24)	−85 (1)	61 (56)	529 (78)
1.25	1.25	2	2134 (39)	4570 (25)	0 (0)	286 (109)	435 (103)	2729 (497)	10154 (517)
1.25	1.25	4	1700 (1)	4008 (3)	0 (0)	558 (248)	46 (66)	−672 (625)	5641 (942)
1.25	1.25	6	844 (2)	7577 (17)	0 (0)	50 (75)	−42 (6)	847 (381)	9278 (447)
1.5	1.5	0	123 (1)	1524 (5)	0 (0)	−128 (39)	−425 (110)	−123 (53)	971 (90)
1.5	1.5	2	3523 (56)	5632 (42)	0 (0)	−1921 (274)	−536 (459)	454 (152)	7151 (595)
1.5	1.5	4	969 (2)	3668 (2)	0 (0)	−252 (92)	203 (146)	268 (516)	4857 (567)
1.5	1.5	6	819 (3)	7406 (11)	0 (0)	−93 (32)	−12 (41)	−285 (5)	7835 (28)
1.75	1.75	0	672 (6)	3230 (10)	0 (0)	−426 (18)	−382 (11)	760 (266)	3854 (252)
1.75	1.75	2	4023 (56)	6674 (50)	0 (0)	−524 (859)	−284 (36)	−4083 (1195)	5806 (294)

1.75 1.75 4	665 (5)	3834 (7)	0 (0)	103 (230)	−31 (128)	349 (193)	4919 (177)
1.75 1.75 6	651 (7)	7039 (1)	0 (0)	82 (161)	−13 (29)	−371 (444)	7388 (261)
2 2 0	891 (7)	5263 (16)	4345341 (35972)	55019 (78016)	−309 (712)	237964 (84969)	4644166 (42190)
2 2 2	3216 (39)	7274 (46)	8674968 (77147)	106995 (152062)	−1028 (272)	−339472 (148817)	8451952 (74181)
2 2 4	641 (10)	4601 (16)	486824 (6850)	6678 (9109)	177 (93)	27835 (6871)	526756 (9064)
2 2 6	398 (7)	6494 (8)	57616 (3758)	703 (835)	−30 (11)	234 (5430)	65414 (2519)
2.25 2.25 0	451 (3)	6771 (21)	0 (0)	−205 (67)	−475 (53)	−1109 (118)	5434 (215)
2.25 2.25 2	1612 (16)	6997 (32)	0 (0)	−273 (19)	−603 (123)	1149 (157)	8881 (283)
2.25 2.25 4	819 (17)	5847 (25)	0 (0)	234 (109)	−106 (48)	7 (892)	6801 (693)
2.25 2.25 6	158 (5)	5863 (12)	0 (0)	6 (6)	−12 (16)	309 (465)	6324 (495)
2.5 2.5 0	5 (0)	7002 (20)	0 (0)	−202 (24)	−1274 (174)	−703 (602)	4828 (424)
2.5 2.5 2	296 (2)	5847 (16)	0 (0)	−3 (7)	−502 (60)	143 (801)	5781 (867)
2.5 2.5 4	1138 (25)	7298 (26)	0 (0)	−588 (60)	−14 (87)	−357 (222)	7477 (24)
2.5 2.5 6	19 (1)	5317 (10)	0 (0)	−4 (2)	22 (12)	−479 (230)	4875 (212)
2.75 2.75 0	471 (2)	6028 (15)	0 (0)	−263 (15)	−114 (88)	−391 (447)	5731 (392)
2.75 2.75 2	52 (1)	4514 (5)	0 (0)	−61 (8)	−190 (59)	−588 (409)	3726 (345)
2.75 2.75 4	1481 (31)	8628 (19)	0 (0)	−133 (317)	−56 (14)	−2117 (738)	7803 (1090)
2.75 2.75 6	12 (1)	5060 (2)	0 (0)	1 (3)	−8 (4)	−272 (693)	4792 (689)
3 3 0	1978 (8)	4910 (7)	2777042 (51014)	683 (193)	−147 (435)	−219811 (10190)	2564653 (40567)
3 3 2	783 (7)	4050 (1)	738846 (12163)	366 (104)	−166 (125)	−26276 (2675)	717603 (9500)
3 3 4	1680 (31)	9531 (8)	552642 (8491)	1025 (387)	−11 (204)	−78491 (27188)	486375 (19326)
3 3 6	104 (0)	5249 (7)	7047 (278)	48 (20)	18 (6)	−2014 (985)	10452 (713)
3.25 3.25 0	3657 (11)	4934 (0)	0 (0)	−432 (229)	2 (7)	867 (51)	9028 (262)
3.25 3.25 2	1711 (13)	5088 (4)	0 (0)	28 (15)	19 (42)	696 (16)	7542 (28)
3.25 3.25 4	1619 (25)	9765 (2)	0 (0)	325 (98)	−12 (8)	1905 (539)	13602 (426)
3.25 3.25 6	230 (2)	5909 (17)	0 (0)	42 (6)	3 (2)	597 (1017)	6782 (1027)
3.5 3.5 0	4430 (9)	6479 (4)	0 (0)	−2195 (277)	−63 (8)	1137 (108)	9788 (372)
3.5 3.5 2	2091 (12)	7211 (9)	0 (0)	−1046 (1)	−136 (35)	−515 (57)	7604 (44)
3.5 3.5 4	1314 (16)	9236 (6)	0 (0)	−295 (63)	99 (3)	824 (890)	11178 (966)
3.5 3.5 6	334 (5)	6898 (22)	0 (0)	−37 (19)	−17 (7)	−757 (461)	6421 (461)
3.75 3.75 0	3909 (4)	8544 (6)	0 (0)	−1069 (1)	−102 (133)	689 (465)	11971 (596)
3.75 3.75 2	1748 (7)	9107 (15)	0 (0)	−409 (216)	−58 (50)	−23 (449)	10364 (162)
3.75 3.75 4	900 (7)	8107 (6)	0 (0)	−126 (110)	−2 (5)	−976 (1294)	7902 (1189)
3.75 3.75 6	391 (7)	7948 (22)	0 (0)	−71 (7)	2 (7)	−281 (335)	7990 (364)

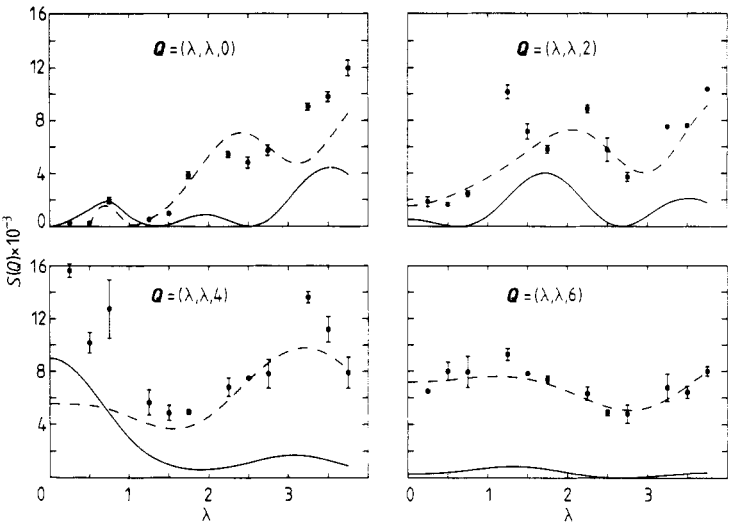

Figure 9. The single-molecule contributions to the total scattering $S(\boldsymbol{Q})$. The full and broken curves correspond to displacement and orientational terms respectively. The data points with error bars are the total scattering amplitudes and are given so that it is possible qualitatively to observe the effects of neighbour correlations. The errors on the single-particle contributions are considerably smaller than for the total scattering and are thus not shown.

that the temperature of the simulation (150 K) is different from that in the experiment (110 K).

(ii) The predominant scattering is from the single-molecule disorder, with the total scattering from the molecular pair correlations rarely exceeding 10% of that of the total scattering. The two single-molecule contributions are shown in figure 9 together with values of the total scattering function. It can be seen that the total single-molecule scattering does not follow the usual form for diffuse scattering from a harmonic crystal (i.e. proportional to $1 - \exp(2W)$, W being the isotropic Debye–Waller factor), consistent with the existence of disorder and anharmonicities.

(iii) The scattering from neighbour correlations is in general either constructive or destructive, dependent on the size of $\boldsymbol{Q}$ and the nature of the correlations.

(iv) The scattering from the correlated orientations S_5 is in general weaker than the scattering from the correlated displacements S_4 (i.e. from the acoustic phonons) and the coupling between the displacements and orientations S_6. It is perhaps surprising that the type of orientational correlations that have been discussed in previous sections does not reveal itself more strongly in the scattering from correlated orientations S_5.

Because these calculations require a large computational effort they have been restricted to the range of $\boldsymbol{Q}$-values described above, and it is clear that the types of correlations that have been studied in the present paper have not really been probed by the total scattering $S(\boldsymbol{Q})$ in this scattering plane. However, it has been the primary purpose here to demonstrate that information about orientational disorder can be obtained from measurements of the total scattering in a coherent neutron scattering experiment. Since what is required is an exploratory search of $\boldsymbol{Q}$-space, larger calculations are probably best left until the corresponding neutron scattering experiment has

been performed. In this case, these calculations would prove invaluable for interpreting the results of such measurements. Moreover, these calculations can also be made for different systems, and we are currently performing such calculations for the orientationally disordered phase of C_2Cl_6 with the aim of trying to understand the origin of the diffuse scattering observed in this crystal.

6. Conclusions

A model that explains the microscopic origin of the orientational disorder in SF_6 has been proposed and tested, and some of the features that are consistent with the dynamic disorder observed have been identified. We now have a sufficiently reasonable understanding of the orientationally disordered phase of SF_6 to enable the calculations to be extended to study the transitions to the low-temperature phases. This work is currently in progress. It is also to be hoped that the results presented here will stimulate further experimental work with SF_6. In particular, it has been shown how information concerning the effects of neighbour orientational correlations can be obtained from coherent neutron scattering experiments.

Acknowledgments

We wish to thank the SERC for financial support, and the staff of the Edinburgh Regional Computer Centre and of the DAP Support Unit, Queen Mary College. One of us (MTD) wishes to thank Dr Werner Press for some helpful comments.

References

Courtens E 1983 *Helv. Phys. Acta* **56** 705
Dolling G, Powell B M and Sears V F 1979 *Mol. Phys.* **37** 1859
Dove M T and Pawley G S 1983 *J. Phys. C: Solid State Phys.* **16** 5969
Fincham D 1983 *Information Quarterly for MD and MC Simulations* (Daresbury Laboratory, UK) **8** 45
Garg S K 1977 *J. Chem. Phys.* **66** 2517
Gerlach P, Prandl W and Lefebvre J 1983 *Mol. Phys.* **49** 991
Gerlach P, Prandl W and Vogt K 1984 *Mol. Phys.* **52** 383
Gilbert M and Drifford M 1972 *Adv. Raman Spectrosc.* **1** 204
Goldstein H 1980 *Classical Mechanics* 2nd edn (Reading, MA: Addison–Wesley)
Hohlwein D 1981 *Acta Crystallogr.* A **37** 899
Kobashi K and Etters R D 1982 *Mol. Phys.* **46** 1077
Michel K 1984 *Z. Phys.* B **54** 129
Pawley G S 1981 *Mol. Phys.* **43** 1321
Pawley G S and Dove M T 1983a *Chem. Phys. Lett.* **99** 45
—— 1983b *Helv. Phys. Acta* **56** 583
Pawley G S and Thomas G W 1982 *Phys. Rev. Lett.* **48** 410
Powles J G, Dore J C, Deraman M B and Osae E K 1983 *Mol. Phys.* **50** 1089
Press W 1981 *Single-Particle Rotations in Molecular Crystals, Springer Tracts in Modern Physics* vol 92 (Berlin: Springer)
Raynerd G, Tatlock G J and Venables J A 1982 *Acta Crystallogr.* B **38** 1896